

VU Research Portal

Observation of $(B)\overline{s}(0) \rightarrow J/\psi f'(2)(1525)$ in $J/\psi K^{(+)}K^{(-)}$ Final States

Aaij, R.; van den Brand, J.F.J.; Dettori, F.; Ketel, T.J.; Lambert, R.W.; Merk, M.H.M.; Raven, H.G.; Schiller, M.

published in

Physical Review Letters
2012

DOI (link to publisher)

[10.1103/PhysRevLett.108.151801](https://doi.org/10.1103/PhysRevLett.108.151801)

document version

Publisher's PDF, also known as Version of record

[Link to publication in VU Research Portal](#)

citation for published version (APA)

Aaij, R., van den Brand, J. F. J., Dettori, F., Ketel, T. J., Lambert, R. W., Merk, M. H. M., Raven, H. G., & Schiller, M. (2012). Observation of $(B)\overline{s}(0) \rightarrow J/\psi f'(2)(1525)$ in $J/\psi K^{(+)}K^{(-)}$ Final States. *Physical Review Letters*, 108(15), [151801]. <https://doi.org/10.1103/PhysRevLett.108.151801>

General rights

Copyright and moral rights for the publications made accessible in the public portal are retained by the authors and/or other copyright owners and it is a condition of accessing publications that users recognise and abide by the legal requirements associated with these rights.

- Users may download and print one copy of any publication from the public portal for the purpose of private study or research.
- You may not further distribute the material or use it for any profit-making activity or commercial gain
- You may freely distribute the URL identifying the publication in the public portal ?

Take down policy

If you believe that this document breaches copyright please contact us providing details, and we will remove access to the work immediately and investigate your claim.

E-mail address:

vuresearchportal.ub@vu.nl

Observation of $\bar{B}_s^0 \rightarrow J/\psi f_2'(1525)$ in $J/\psi K^+ K^-$ Final States

R. Aaij,²³ C. Abellan Beteta,^{35,n} B. Adeva,³⁶ M. Adinolfi,⁴² C. Adrover,⁶ A. Affolder,⁴⁸ Z. Ajaltouni,⁵ J. Albrecht,³⁷ F. Alessio,³⁷ M. Alexander,⁴⁷ G. Alkhazov,²⁹ P. Alvarez Cartelle,³⁶ A. A. Alves Jr,²² S. Amato,² Y. Amhis,³⁸ J. Anderson,³⁹ R. B. Appleby,⁵⁰ O. Aquines Gutierrez,¹⁰ F. Archilli,^{18,37} L. Arrabito,⁵³ A. Artamonov,³⁴ M. Artuso,^{52,37} E. Aslanides,⁶ G. Auriemma,^{22,m} S. Bachmann,¹¹ J. J. Back,⁴⁴ D. S. Bailey,⁵⁰ V. Balagura,^{30,37} W. Baldini,¹⁶ R. J. Barlow,⁵⁰ C. Barschel,³⁷ S. Barsuk,⁷ W. Barter,⁴³ A. Bates,⁴⁷ C. Bauer,¹⁰ Th. Bauer,²³ A. Bay,³⁸ I. Bediaga,¹ S. Belogurov,³⁰ K. Belous,³⁴ I. Belyaev,^{30,37} E. Ben-Haim,⁸ M. Benayoun,⁸ G. Bencivenni,¹⁸ S. Benson,⁴⁶ J. Benton,⁴² R. Bernet,³⁹ M.-O. Bettler,¹⁷ M. van Beuzekom,²³ A. Bien,¹¹ S. Bifani,¹² T. Bird,⁵⁰ A. Bizzeti,^{17,h} P. M. Bjørnstad,⁵⁰ T. Blake,³⁷ F. Blanc,³⁸ C. Blanks,⁴⁹ J. Blouw,¹¹ S. Blusk,⁵² A. Bobrov,³³ V. Bocci,²² A. Bondar,³³ N. Bondar,²⁹ W. Bonivento,¹⁵ S. Borghi,^{47,50} A. Borgia,⁵² T. J. V. Bowcock,⁴⁸ C. Bozzi,¹⁶ T. Brambach,⁹ J. van den Brand,²⁴ J. Bressieux,³⁸ D. Brett,⁵⁰ M. Britsch,¹⁰ T. Britton,⁵² N. H. Brook,⁴² H. Brown,⁴⁸ A. Büchler-Germann,³⁹ I. Burducea,²⁸ A. Bursche,³⁹ J. Buytaert,³⁷ S. Cadeddu,¹⁵ O. Callot,⁷ M. Calvi,^{20,j} M. Calvo Gomez,^{35,n} A. Camboni,³⁵ P. Campana,^{18,37} A. Carbone,¹⁴ G. Carboni,^{21,i} R. Cardinale,^{19,37,i} A. Cardini,¹⁵ L. Carson,⁴⁹ K. Carvalho Akiba,² G. Casse,⁴⁸ M. Cattaneo,³⁷ Ch. Cauet,⁹ M. Charles,⁵¹ Ph. Charpentier,³⁷ N. Chiapolini,³⁹ K. Ciba,³⁷ X. Cid Vidal,³⁶ G. Ciezarek,⁴⁹ P. E. L. Clarke,^{46,37} M. Clemencic,³⁷ H. V. Cliff,⁴³ J. Closier,³⁷ C. Coca,²⁸ V. Coco,²³ J. Cogan,⁶ P. Collins,³⁷ A. Comerma-Montells,³⁵ F. Constantin,²⁸ A. Contu,⁵¹ A. Cook,⁴² M. Coombes,⁴² G. Corti,³⁷ G. A. Cowan,³⁸ R. Currie,⁴⁶ C. D'Ambrosio,³⁷ P. David,⁸ P. N. Y. David,²³ I. De Bonis,⁴ S. De Capua,^{21,k} M. De Cian,³⁹ F. De Lorenzi,¹² J. M. De Miranda,¹ L. De Paula,² P. De Simone,¹⁸ D. Decamp,⁴ M. Deckenhoff,⁹ H. Degaudenzi,^{38,37} L. Del Buono,⁸ C. Deplano,¹⁵ D. Derkach,^{14,37} O. Deschamps,⁵ F. Dettori,²⁴ J. Dickens,⁴³ H. Dijkstra,³⁷ P. Diniz Batista,¹ F. Domingo Bonal,^{35,n} S. Donleavy,⁴⁸ F. Dordei,¹¹ A. Dosil Suárez,³⁶ D. Dossett,⁴⁴ A. Dovbnya,⁴⁰ F. Dupertuis,³⁸ R. Dzhelyadin,³⁴ A. Dziurda,²⁵ S. Easo,⁴⁵ U. Egede,⁴⁹ V. Egorychev,³⁰ S. Eidelman,³³ D. van Eijk,²³ F. Eisele,¹¹ S. Eisenhardt,⁴⁶ R. Ekelhof,⁹ L. Eklund,⁴⁷ Ch. Elsasser,³⁹ D. Elsby,⁵⁵ D. Esperante Pereira,³⁶ L. Estève,⁴³ A. Falabella,^{16,14,e} E. Fanchini,^{20,j} C. Färber,¹¹ G. Fardell,⁴⁶ C. Farinelli,²³ S. Farry,¹² V. Fave,³⁸ V. Fernandez Albor,³⁶ M. Ferro-Luzzi,³⁷ S. Filippov,³² C. Fitzpatrick,⁴⁶ M. Fontana,¹⁰ F. Fontanelli,^{19,i} R. Forty,³⁷ M. Frank,³⁷ C. Frei,³⁷ M. Frosini,^{17,37,f} S. Furcas,²⁰ A. Gallas Torreira,³⁶ D. Galli,^{14,c} M. Gandelman,² P. Gandini,⁵¹ Y. Gao,³ J.-C. Garnier,³⁷ J. Garofoli,⁵² J. Garra Tico,⁴³ L. Garrido,³⁵ D. Gascon,³⁵ C. Gaspar,³⁷ N. Gauvin,³⁸ M. Gersabeck,³⁷ T. Gershon,^{44,37} Ph. Ghez,⁴ V. Gibson,⁴³ V. V. Gligorov,³⁷ C. Göbel,⁵⁴ D. Golubkov,³⁰ A. Golutvin,^{49,30,37} A. Gomes,² H. Gordon,⁵¹ M. Grabalosa Gándara,³⁵ R. Graciani Diaz,³⁵ L. A. Granado Cardoso,³⁷ E. Graugés,³⁵ G. Graziani,¹⁷ A. Grecu,²⁸ E. Greening,⁵¹ S. Gregson,⁴³ B. Gui,⁵² E. Gushchin,³² Yu. Guz,³⁴ T. Gys,³⁷ G. Haefeli,³⁸ C. Haen,³⁷ S. C. Haines,⁴³ T. Hampson,⁴² S. Hansmann-Menzemer,¹¹ R. Harji,⁴⁹ N. Harnew,⁵¹ J. Harrison,⁵⁰ P. F. Harrison,⁴⁴ T. Hartmann,⁵⁶ J. He,⁷ V. Heijne,²³ K. Hennessy,⁴⁸ P. Henrard,⁵ J. A. Hernandez Morata,³⁶ E. van Herwijnen,³⁷ E. Hicks,⁴⁸ K. Holubyev,¹¹ P. Hopchev,⁴ W. Hulsbergen,²³ P. Hunt,⁵¹ T. Huse,⁴⁸ R. S. Huston,¹² D. Hutchcroft,⁴⁸ D. Hynds,⁴⁷ V. Iakovenko,⁴¹ P. Ilten,¹² J. Imong,⁴² R. Jacobsson,³⁷ A. Jaeger,¹¹ M. Jahjah Hussein,⁵ E. Jans,²³ F. Jansen,²³ P. Jaton,³⁸ B. Jean-Marie,⁷ F. Jing,³ M. John,⁵¹ D. Johnson,⁵¹ C. R. Jones,⁴³ B. Jost,³⁷ M. Kaballo,⁹ S. Kandybei,⁴⁰ M. Karacson,³⁷ T. M. Karbach,⁹ J. Keaveney,¹² I. R. Kenyon,⁵⁵ U. Kerzel,³⁷ T. Ketel,²⁴ A. Keune,³⁸ B. Khanji,⁶ Y. M. Kim,⁴⁶ M. Knecht,³⁸ P. Koppenburg,²³ A. Kozlinskiy,²³ L. Kravchuk,³² K. Kreplin,¹¹ M. Kreps,⁴⁴ G. Krocker,¹¹ P. Krokovny,¹¹ F. Kruse,⁹ K. Kruzelecki,³⁷ M. Kucharczyk,^{20,25,37,j} T. Kvaratskheliya,^{30,37} V. N. La Thi,³⁸ D. Lacarrere,³⁷ G. Lafferty,⁵⁰ A. Lai,¹⁵ D. Lambert,⁴⁶ R. W. Lambert,²⁴ E. Lanciotti,³⁷ G. Lanfranchi,¹⁸ C. Langenbruch,¹¹ T. Latham,⁴⁴ C. Lazzeroni,⁵⁵ R. Le Gac,⁶ J. van Leerdam,²³ J.-P. Lees,⁴ R. Lefèvre,⁵ A. Leflat,^{31,37} J. Lefrançois,⁷ O. Leroy,⁶ T. Lesiak,²⁵ L. Li,³ L. Li Gioi,⁵ M. Lieng,⁹ M. Liles,⁴⁸ R. Lindner,³⁷ C. Linn,¹¹ B. Liu,³ G. Liu,³⁷ J. von Loeben,²⁰ J. H. Lopes,² E. Lopez Asamar,³⁵ N. Lopez-March,³⁸ H. Lu,^{38,3} J. Luisier,³⁸ A. Mac Raighne,⁴⁷ F. Machefert,⁷ I. V. Machikhiliyan,^{4,30} F. Maciuc,¹⁰ O. Maev,^{29,37} J. Magnin,¹ S. Malde,⁵¹ R. M. D. Mamunur,³⁷ G. Manca,^{15,d} G. Mancinelli,⁶ N. Mangiafave,⁴³ U. Marconi,¹⁴ R. Märki,³⁸ J. Marks,¹¹ G. Martellotti,²² A. Martens,⁸ L. Martin,⁵¹ A. Martín Sánchez,⁷ D. Martinez Santos,³⁷ A. Massafferri,¹ Z. Mathe,¹² C. Matteuzzi,²⁰ M. Matveev,²⁹ E. Maurice,⁶ B. Maynard,⁵² A. Mazurov,^{16,32,37} G. McGregor,⁵⁰ R. McNulty,¹² M. Meissner,¹¹ M. Merk,²³ J. Merkel,⁹ R. Messi,^{21,k} S. Miglioranza,³⁷ D. A. Milanes,^{13,37} M.-N. Minard,⁴ J. Molina Rodriguez,⁵⁴ S. Monteil,⁵ D. Moran,¹² P. Morawski,²⁵ R. Mountain,⁵² I. Mous,²³ F. Muheim,⁴⁶ K. Müller,³⁹ R. Muresan,^{28,38} B. Muryn,²⁶ B. Muster,³⁸ M. Musy,³⁷ J. Mylroie-Smith,⁴⁸ P. Naik,⁴² T. Nakada,³⁸ R. Nandakumar,⁴⁵ I. Nasteva,¹ M. Nedos,⁹ M. Needham,⁴⁶ N. Neufeld,³⁷ C. Nguyen-Mau,^{38,o} M. Nicol,⁷ V. Niess,⁵ N. Nikitin,³¹ A. Nomerotski,⁵¹ A. Novoselov,³⁴ A. Oblakowska-Mucha,²⁶ V. Obraztsov,³⁴ S. Oggero,²³ S. Ogilvy,⁴⁷ O. Okhrimenko,⁴¹ R. Oldeman,^{15,d} M. Orlandea,²⁸ J. M. Otalora Goicochea,²

P. Owen,⁴⁹ B. Pal,⁵² J. Palacios,³⁹ A. Palano,^{13,b} M. Palutan,¹⁸ J. Panman,³⁷ A. Papanestis,⁴⁵ M. Pappagallo,⁴⁷ C. Parkes,^{50,37} C. J. Parkinson,⁴⁹ G. Passaleva,¹⁷ G. D. Patel,⁴⁸ M. Patel,⁴⁹ S. K. Paterson,⁴⁹ G. N. Patrick,⁴⁵ C. Patrignani,^{19,i} C. Pavel-Nicorescu,²⁸ A. Pazos Alvarez,³⁶ A. Pellegrino,²³ G. Penso,^{22,l} M. Pepe Altarelli,³⁷ S. Perazzini,^{14,c} D. L. Perego,^{20,j} E. Perez Trigo,³⁶ A. Pérez-Calero Yzquierdo,³⁵ P. Perret,⁵ M. Perrin-Terrin,⁶ G. Pessina,²⁰ A. Petrella,^{16,37} A. Petrolini,^{19,i} A. Phan,⁵² E. Picatoste Olloqui,³⁵ B. Pie Valls,³⁵ B. Pietrzyk,⁴ T. Pilař,⁴⁴ D. Pinci,²² R. Plackett,⁴⁷ S. Playfer,⁴⁶ M. Plo Casasus,³⁶ G. Polok,²⁵ A. Poluektov,^{44,33} E. Polycarpo,² D. Popov,¹⁰ B. Popovici,²⁸ C. Potterat,³⁵ A. Powell,⁵¹ J. Prisciandaro,³⁸ V. Pugatch,⁴¹ A. Puig Navarro,³⁵ W. Qian,⁵² J. H. Rademacker,⁴² B. Rakotomiamanana,³⁸ M. S. Rangel,² I. Raniuk,⁴⁰ G. Raven,²⁴ S. Redford,⁵¹ M. M. Reid,⁴⁴ A. C. dos Reis,¹ S. Ricciardi,⁴⁵ K. Rinnert,⁴⁸ D. A. Roa Romero,⁵ P. Robbe,⁷ E. Rodrigues,^{47,50} F. Rodrigues,² P. Rodriguez Perez,³⁶ G. J. Rogers,⁴³ S. Roiser,³⁷ V. Romanovsky,³⁴ M. Rosello,^{35,n} J. Rouvinet,³⁸ T. Ruf,³⁷ H. Ruiz,³⁵ G. Sabatino,^{21,k} J. J. Saborido Silva,³⁶ N. Sagidova,²⁹ P. Sail,⁴⁷ B. Saitta,^{15,d} C. Salzmann,³⁹ M. Sannino,^{19,i} R. Santacesaria,²² C. Santamarina Rios,³⁶ R. Santinelli,³⁷ E. Santovetti,^{21,k} M. Sapunov,⁶ A. Sarti,^{18,l} C. Satriano,^{22,m} A. Satta,²¹ M. Savrie,^{16,e} D. Savrina,³⁰ P. Schaack,⁴⁹ M. Schiller,²⁴ S. Schleich,⁹ M. Schlupp,⁹ M. Schmelling,¹⁰ B. Schmidt,³⁷ O. Schneider,³⁸ A. Schopper,³⁷ M.-H. Schune,⁷ R. Schwemmer,³⁷ B. Sciascia,¹⁸ A. Sciubba,^{18,l} M. Seco,³⁶ A. Semennikov,³⁰ K. Senderowska,²⁶ I. Sepp,⁴⁹ N. Serra,³⁹ J. Serrano,⁶ P. Seyfert,¹¹ M. Shapkin,³⁴ I. Shapoval,^{40,37} P. Shatalov,³⁰ Y. Shcheglov,²⁹ T. Shears,⁴⁸ L. Shekhtman,³³ O. Shevchenko,⁴⁰ V. Shevchenko,³⁰ A. Shires,⁴⁹ R. Silva Coutinho,⁴⁴ T. Skwarnicki,⁵² A. C. Smith,³⁷ N. A. Smith,⁴⁸ E. Smith,^{51,45} K. Sobczak,⁵ F. J. P. Soler,⁴⁷ A. Solomin,⁴² F. Soomro,¹⁸ B. Souza De Paula,² B. Spaan,⁹ A. Sparkes,⁴⁶ P. Spradlin,⁴⁷ F. Stagni,³⁷ S. Stahl,¹¹ O. Steinkamp,³⁹ S. Stoica,²⁸ S. Stone,^{52,37} B. Storaci,²³ M. Straticiuc,²⁸ U. Straumann,³⁹ V. K. Subbiah,³⁷ S. Swientek,⁹ M. Szczekowski,²⁷ P. Szczypka,³⁸ T. Szumlak,²⁶ S. T'Jampens,⁴ E. Teodorescu,²⁸ F. Teubert,³⁷ C. Thomas,⁵¹ E. Thomas,³⁷ J. van Tilburg,¹¹ V. Tisserand,⁴ M. Tobin,³⁹ S. Topp-Joergensen,⁵¹ N. Torr,⁵¹ E. Tournefier,^{4,49} M. T. Tran,³⁸ A. Tsaregorodtsev,⁶ N. Tuning,²³ M. Ubeda Garcia,³⁷ A. Ukleja,²⁷ P. Urquijo,⁵² U. Uwer,¹¹ V. Vagnoni,¹⁴ G. Valenti,¹⁴ R. Vazquez Gomez,³⁵ P. Vazquez Regueiro,³⁶ S. Vecchi,¹⁶ J. J. Velthuis,⁴² M. Veltri,^{17,g} B. Viaud,⁷ I. Videau,⁷ X. Vilasis-Cardona,^{35,n} J. Visniakov,³⁶ A. Vollhardt,³⁹ D. Volyanskyy,¹⁰ D. Voong,⁴² A. Vorobyev,²⁹ H. Voss,¹⁰ S. Wandernoth,¹¹ J. Wang,⁵² D. R. Ward,⁴³ N. K. Watson,⁵⁵ A. D. Webber,⁵⁰ D. Websdale,⁴⁹ M. Whitehead,⁴⁴ D. Wiedner,¹¹ L. Wiggers,²³ G. Wilkinson,⁵¹ M. P. Williams,^{44,45} M. Williams,⁴⁹ F. F. Wilson,⁴⁵ J. Wishahi,⁹ M. Witek,²⁵ W. Witzeling,³⁷ S. A. Wotton,⁴³ K. Wyllie,³⁷ Y. Xie,⁴⁶ F. Xing,⁵¹ Z. Xing,⁵² Z. Yang,³ R. Young,⁴⁶ O. Yushchenko,³⁴ M. Zavertyaev,^{10,a} F. Zhang,³ L. Zhang,⁵² W. C. Zhang,¹² Y. Zhang,³ A. Zhelezov,¹¹ L. Zhong,³ E. Zverev,³¹ and A. Zvyagin³⁷

(The LHCb Collaboration)

¹Centro Brasileiro de Pesquisas Físicas (CBPF), Rio de Janeiro, Brazil

²Universidade Federal do Rio de Janeiro (UFRJ), Rio de Janeiro, Brazil

³Center for High Energy Physics, Tsinghua University, Beijing, China

⁴LAPP, Université de Savoie, CNRS/IN2P3, Annecy-Le-Vieux, France

⁵Clermont Université, Université Blaise Pascal, CNRS/IN2P3, LPC, Clermont-Ferrand, France

⁶CPM, Aix-Marseille Université, CNRS/IN2P3, Marseille, France

⁷LAL, Université Paris-Sud, CNRS/IN2P3, Orsay, France

⁸LPNHE, Université Pierre et Marie Curie, Université Paris Diderot, CNRS/IN2P3, Paris, France

⁹Fakultät Physik, Technische Universität Dortmund, Dortmund, Germany

¹⁰Max-Planck-Institut für Kernphysik (MPIK), Heidelberg, Germany

¹¹Physikalisches Institut, Ruprecht-Karls-Universität Heidelberg, Heidelberg, Germany

¹²School of Physics, University College Dublin, Dublin, Ireland

¹³Sezione INFN di Bari, Bari, Italy

¹⁴Sezione INFN di Bologna, Bologna, Italy

¹⁵Sezione INFN di Cagliari, Cagliari, Italy

¹⁶Sezione INFN di Ferrara, Ferrara, Italy

¹⁷Sezione INFN di Firenze, Firenze, Italy

¹⁸Laboratori Nazionali dell'INFN di Frascati, Frascati, Italy

¹⁹Sezione INFN di Genova, Genova, Italy

²⁰Sezione INFN di Milano Bicocca, Milano, Italy

²¹Sezione INFN di Roma Tor Vergata, Roma, Italy

²²Sezione INFN di Roma La Sapienza, Roma, Italy

²³Nikhef National Institute for Subatomic Physics, Amsterdam, The Netherlands

- ²⁴*Nikhef National Institute for Subatomic Physics and Vrije Universiteit, Amsterdam, The Netherlands*
²⁵*Henryk Niewodniczanski Institute of Nuclear Physics Polish Academy of Sciences, Kraków, Poland*
²⁶*AGH University of Science and Technology, Kraków, Poland*
²⁷*Soltan Institute for Nuclear Studies, Warsaw, Poland*
²⁸*Horia Hulubei National Institute of Physics and Nuclear Engineering, Bucharest-Magurele, Romania*
²⁹*Petersburg Nuclear Physics Institute (PNPI), Gatchina, Russia*
³⁰*Institute of Theoretical and Experimental Physics (ITEP), Moscow, Russia*
³¹*Institute of Nuclear Physics, Moscow State University (SINP MSU), Moscow, Russia*
³²*Institute for Nuclear Research of the Russian Academy of Sciences (INR RAN), Moscow, Russia*
³³*Budker Institute of Nuclear Physics (SB RAS) and Novosibirsk State University, Novosibirsk, Russia*
³⁴*Institute for High Energy Physics (IHEP), Protvino, Russia*
³⁵*Universitat de Barcelona, Barcelona, Spain*
³⁶*Universidad de Santiago de Compostela, Santiago de Compostela, Spain*
³⁷*European Organization for Nuclear Research (CERN), Geneva, Switzerland*
³⁸*Ecole Polytechnique Fédérale de Lausanne (EPFL), Lausanne, Switzerland*
³⁹*Physik-Institut, Universität Zürich, Zürich, Switzerland*
⁴⁰*NSC Kharkiv Institute of Physics and Technology (NSC KIPT), Kharkiv, Ukraine*
⁴¹*Institute for Nuclear Research of the National Academy of Sciences (KINR), Kyiv, Ukraine*
⁴²*H. H. Wills Physics Laboratory, University of Bristol, Bristol, United Kingdom*
⁴³*Cavendish Laboratory, University of Cambridge, Cambridge, United Kingdom*
⁴⁴*Department of Physics, University of Warwick, Coventry, United Kingdom*
⁴⁵*STFC Rutherford Appleton Laboratory, Didcot, United Kingdom*
⁴⁶*School of Physics and Astronomy, University of Edinburgh, Edinburgh, United Kingdom*
⁴⁷*School of Physics and Astronomy, University of Glasgow, Glasgow, United Kingdom*
⁴⁸*Oliver Lodge Laboratory, University of Liverpool, Liverpool, United Kingdom*
⁴⁹*Imperial College London, London, United Kingdom*
⁵⁰*School of Physics and Astronomy, University of Manchester, Manchester, United Kingdom*
⁵¹*Department of Physics, University of Oxford, Oxford, United Kingdom*
⁵²*Syracuse University, Syracuse, New York, USA*
⁵³*CC-IN2P3, CNRS/IN2P3, Lyon-Villeurbanne, France, associated member*
⁵⁴*Pontifícia Universidade Católica do Rio de Janeiro (PUC-Rio), Rio de Janeiro, Brazil, associated to, Universidade Federal do Rio de Janeiro (UFRJ), Rio de Janeiro, Brazil*
⁵⁵*University of Birmingham, Birmingham, United Kingdom*
⁵⁶*Physikalisches Institut, Universität Rostock, Rostock, Germany, associated to, Physikalisches Institut, Ruprecht-Karls-Universität Heidelberg, Heidelberg, Germany*
(Received 20 December 2011; published 9 April 2012)

The decay $\bar{B}_s^0 \rightarrow J/\psi K^+ K^-$ is investigated using 0.16 fb^{-1} of data collected with the LHCb detector using 7 TeV pp collisions. Although the $J/\psi \phi$ channel is well known, final states at higher $K^+ K^-$ masses have not previously been studied. In the $K^+ K^-$ mass spectrum we observe a significant signal in the $f_2'(1525)$ region as well as a nonresonant component. After subtracting the nonresonant component, we find $\mathcal{B}(\bar{B}_s^0 \rightarrow J/\psi f_2'(1525))/\mathcal{B}(\bar{B}_s^0 \rightarrow J/\psi \phi) = (26.4 \pm 2.7 \pm 2.4)\%$.

DOI: 10.1103/PhysRevLett.108.151801

PACS numbers: 13.25.Hw, 14.40.Nd, 14.40.Be

The $\bar{B}_s^0 \rightarrow J/\psi K^+ K^-$ channel has previously been studied only when the $K^+ K^-$ are consistent with the decay of the ϕ meson. This mode has been used to measure the CP violation in \bar{B}_s^0 mixing, ϕ_s , a key probe in the search for physics beyond the standard model [1–4] (Charge conjugate modes are also considered throughout). In addition to the ϕ other resonant or nonresonant final states may appear and affect the CP measurements, including an

S -wave contribution [5]. In this Letter, we study the entire $K^+ K^-$ mass spectrum, including a search for other final states that may be useful in CP violation studies. These states may provide other ways of measuring ϕ_s , in decays with a different spin structure that may be useful for revealing different aspects of CP violation.

We use a 0.16 fb^{-1} data sample collected with the LHCb detector [6] at a center-of-mass energy of 7 TeV. The detector elements most important for this analysis include a vertex locator, a silicon strip device that surrounds the pp interaction region in the LHC, and other downstream tracking devices before and after a 4 Tm dipole magnet. Two ring-imaging Cherenkov detectors are used to identify charged hadrons, while muons are identified using their

penetration through iron. This analysis is restricted to events accepted by a dimuon trigger [7]. Subsequent selection criteria are applied that serve to reject background, yet preserve high efficiencies, as determined by Monte Carlo (MC) events generated using PYTHIA [8], and the LHCb detector simulation based on GEANT [9]. To be considered as a $J/\psi \rightarrow \mu^+ \mu^-$ candidate, opposite sign tracks are required to have transverse momentum, p_T , greater than 500 MeV, be identified as muons, and give a good fit to a common vertex. (We work in units where $c = 1$.) Dimuon candidates with masses between -48 and $+43$ MeV of the J/ψ peak are selected for further analysis, where the rms resolution is 13.4 MeV. The invariant mass of the $\mu^+ \mu^-$ pair is constrained to the J/ψ mass for further analysis.

Kaon candidates are selected if their minimum distance from the closest primary vertex is inconsistent with being produced at that vertex. They must be positively identified based on the logarithm of the likelihood ratio comparing two particle hypotheses (DLL). There are two criteria used: loose corresponds to $\text{DLL}(K - \pi) > 0$, while tight has $\text{DLL}(K - \pi) > 10$ and $\text{DLL}(K - p) > -3$. We use the loose criterion for checking kaon identification efficiencies, otherwise the tight criterion is used. In addition, the two kaons must have the sum of the magnitudes of their $p_T > 900$ MeV.

To select \bar{B}_s^0 candidates we require that the $K^+ K^-$ pair and the J/ψ candidate give a good fit to a common secondary vertex with a $\chi^2 < 5$ per degree of freedom. We also require that the \bar{B}_s^0 candidate's decay point must be > 1.5 mm from the primary vertex and that the negative of its momentum vector points back to the primary.

The \bar{B}_s^0 candidate invariant mass is shown in Fig. 1. A clear signal is seen, part of which comes from the previously known $J/\psi \phi$ mode. A check was made for possible resonant states decaying to $J/\psi K^-$ since similar exotic states have been claimed [10], but no obvious structures are

visible in the invariant mass spectrum. Figure 2 shows the $K^+ K^-$ invariant mass for both signal and sideband regions, where the signal region extends ± 25 MeV around the \bar{B}_s^0 mass peak and the sidebands extend from 35 to 60 MeV on either side of the peak. Apart from the large peak at the ϕ , there is a structure near 1525 MeV. In addition there is an excess of signal events over most of the mass range which we refer to as nonresonant. We investigate the possibility of the peak to be the $f_2'(1525)$ resonance. The PDG quotes the mass of the f_2' state as 1525 ± 5 MeV and the width as 73_{-5}^{+6} MeV [11]. Other states such as the $f_2(1270)$ and the $f_0(1500)$ have small branching fractions into $K^+ K^-$ of less than 5%, and are unlikely to have large rates.

It is possible for the decay $\bar{B}^0 \rightarrow J/\psi K^- \pi^+$ to fake our signal if the π^+ is misidentified as a K^+ . A specific example is given by $\bar{B}^0 \rightarrow J/\psi \bar{K}_2^*(1430)$ decays [12]. To examine if we are sensitive to a reflection of this mode in the 1525 MeV dikaon mass region, a simulation was performed where the π^+ from the $\bar{K}_2^*(1430)$ was interpreted as a K^+ . Figure 3(a) shows that the reflection of this mode does indeed peak in the dikaon mass range around 1525 MeV. It also peaks in the \bar{B}_s^0 signal region but is much wider than the \bar{B}_s^0 mass peak. The region 25–200 MeV above the \bar{B}_s^0 mass peak provides a sample of misidentified $\bar{B}^0 \rightarrow J/\psi K^- \pi^+$ decays. By measuring the number of \bar{B}^0 candidates in this region we can calculate the number in the \bar{B}_s^0 signal region.

To determine the size of any \bar{B}^0 reflection in the f_2' mass region we select events where the reconstructed $J/\psi K^+ K^-$ mass is in the range 25–200 MeV above the \bar{B}_s^0 mass, reassign each of the two kaons in turn to the pion hypothesis, and plot the $J/\psi K \pi$ mass. The resulting peak at the \bar{B}^0 mass has 36 ± 10 events from the fit shown in Fig. 3(b). We calculate 37 ± 10 events in the \bar{B}_s^0 signal region, using the shape from Monte Carlo simulation, and use this number as a constraint in the fit described below to determine the f_2' parameters and signal yields.

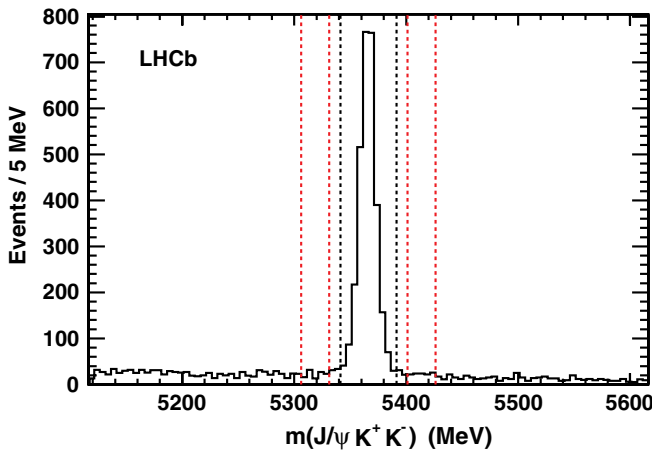


FIG. 1 (color online). Invariant mass of $J/\psi K^+ K^-$ combinations. The vertical lines indicate the signal and sideband regions.

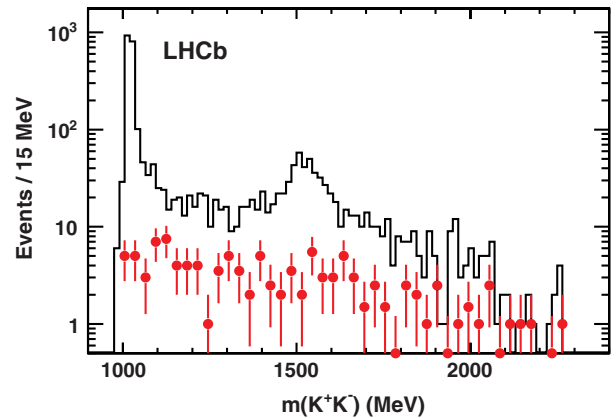


FIG. 2 (color online). Invariant mass of $K^+ K^-$ combinations. The histogram shows the data in the signal region while the points (red) show the sidebands.

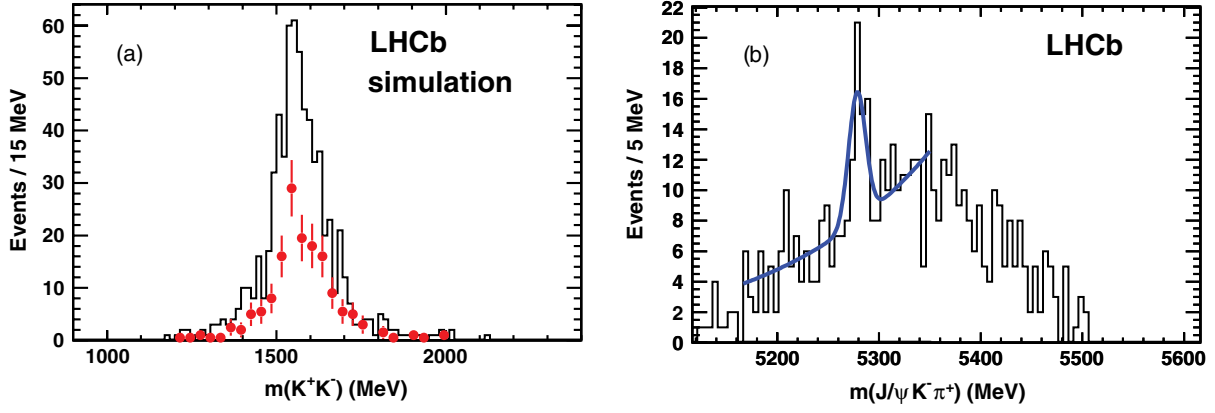


FIG. 3 (color online). (a) The $m(K^+K^-)$ distribution for simulated $\bar{B}^0 \rightarrow J/\psi \bar{K}_2^*(1430)$ decays where the π^+ from the $\bar{K}_2^*(1430)$ decay is interpreted as a K^+ . The histogram shows $m(K^+K^-)$ in the signal region of \bar{B}_s^0 mass and the points in the sideband region. The simulation corresponds to approximately 8 fb^{-1} of data. (b) The $m(J/\psi K^+K^-)$ distribution for $J/\psi K^+K^-$ data candidates 25–200 MeV above the \bar{B}_s^0 mass, and with $m(K^+K^-)$ within ± 300 MeV of 1525 MeV, reinterpreted as $\bar{B}^0 \rightarrow J/\psi K^- \pi^+$ events. The fit is to a signal Gaussian whose mass and width are allowed to vary as well as a quadratic background.

To test the f_2' hypothesis we perform a simultaneous fit to the \bar{B}_s^0 candidate mass and the dikaon mass. The f_2' signal is parametrized by a spin-2 Breit-Wigner function [13]. The width of the f_2' is fixed to the PDG value of 73 MeV [11]. A contribution from nonresonant K^+K^- is included as a linear function in the dikaon mass. The contribution from the $K^- \pi^+$ reflection is included using the dikaon and \bar{B}_s^0 mass shapes from the simulation, with the normalization fixed by the event yield in Fig. 3(b). The results of the fits are shown in Fig. 4. The f_2' mass from the fit is 1525 ± 4 MeV and the yield is 269 ± 26 events within ± 125 MeV of the mass. If we allow the f_2' width to vary we find a consistent value of 90^{+16}_{-14} MeV. As we have not taken into account possible interferences between the f_2' and other $J/\psi K^+K^-$ final states we do not provide systematic uncertainties for these values. The decay angle of the J/ψ , $\theta_{J/\psi}$, can test for pure spin 0, or the presence of a higher spin state such as the spin-2 f_2' [11]. Here $\theta_{J/\psi}$ is

defined as the angle of the μ^+ with respect to the \bar{B}_s^0 direction in the J/ψ rest frame. It is distributed as

$$f(\cos\theta_{J/\psi}) = (1 - p)\sin^2\theta_{J/\psi} + \frac{p}{2}(1 + \cos^2\theta_{J/\psi}), \quad (1)$$

where $1 - p$ is the fraction of helicity zero and p is the fraction of helicity ± 1 . Shown in Fig. 5 is the background subtracted, acceptance corrected $\cos\theta_{J/\psi}$ distribution for K^+K^- masses in the f_2' region. MC simulation is used to find the acceptance correction. The points are extracted from the joint fit to the $m(J/\psi K^+K^-)$ and $m(K^+K^-)$ distributions in the K^+K^- mass region within 1400–1650 MeV for events in the peak above the nonresonant K^+K^- . The fit result is $p = (0.57 \pm 0.13)$, with $\chi^2/\text{number of degrees of freedom (ndof)}$ of 10/8 (27% probability). Fitting only with an S wave gives χ^2/ndof of 27/9 (0.1% probability), showing that the data are not

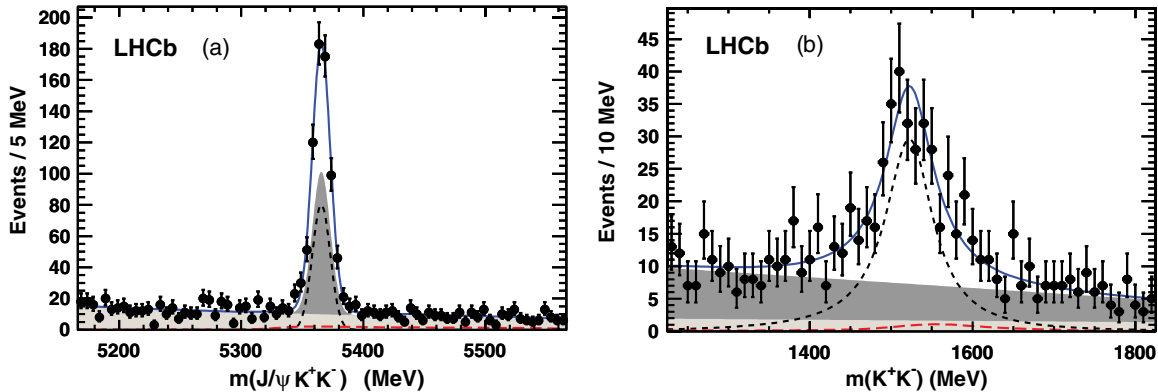


FIG. 4 (color online). Projections of fits to (a) the \bar{B}_s^0 candidate mass and (b) the dikaon mass. The f_2' signal is parametrized by a spin-2 Breit-Wigner function whose width is fixed to 73 MeV (dotted curve). The combinatorial background is shown in the light shaded region, while the darker shaded region shows the nonresonant $J/\psi K^+K^-$ component. The long-dashed (red) line shows the misidentified $\bar{B}^0 \rightarrow J/\psi K^- \pi^+$ decays, and the (blue) line the total.

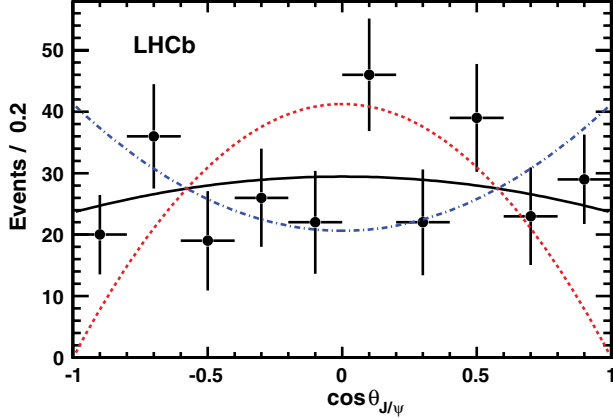


FIG. 5 (color online). Distribution of $\cos\theta_{J/\psi}$ for $\bar{B}_s^0 \rightarrow J/\psi f_2'$ decays. The background and nonresonant K^+K^- components have been subtracted, and the data have been corrected for acceptance. The fit to Eq. (1) is shown by the solid line. Note that for pure S wave the distribution would be $\sin^2\theta_{J/\psi}$ ($p=0$), shown as the dotted curve, while for pure helicity 1 ($p=1$) the data would be described by the dotted-dashed curve.

likely to be pure spin 0, but are compatible with a higher spin state consistent with an f_2' contribution.

The branching fraction of $\bar{B}_s^0 \rightarrow J/\psi f_2'$ relative to $\bar{B}_s^0 \rightarrow J/\psi \phi$ is determined by assuming that the dominant background is S wave and the signal D wave, so there is no interference between them (Although there can be interference as a function of the K^+ decay angle in the f_2' rest frame, integrating over this variable causes the net result to be zero). The number of $J/\psi K^+K^-$ events is determined by a fit to the \bar{B}_s^0 mass distribution, within ± 20 MeV of the ϕ mass. A small S -wave component in the ϕ mass region of $(4.2 \pm 2.3)\%$ is subtracted [2]. Although there are the same final state particles in both modes, the relative efficiency is $(78 \pm 2)\%$, where the uncertainty arises from simulation statistics. The efficiency ratio differs from unity due to the different p_T distributions of the kaons in the final states. The kaon identification efficiencies are corrected with respect to those given by the MC simulation using a sample of D^{*+} decays, where the kaon can be selected without resorting to particle identification (PID) information. Typical corrections are on the order of 5%.

To find the effective relative rate of f_2' decays we use the fit where the width is allowed to vary. There are 320 ± 33 f_2' events and 1774 ± 42 ϕ events. Correcting for the relative efficiencies and the explicit branching fractions $\mathcal{B}(f_2'(1525) \rightarrow K^+K^-) = (44.4 \pm 1.1)\%$, and $\mathcal{B}(\phi \rightarrow K^+K^-) = (48.9 \pm 0.5)\%$ [11], we measure

$$R \equiv \frac{\mathcal{B}(\bar{B}_s^0 \rightarrow J/\psi f_2'(1525))}{\mathcal{B}(\bar{B}_s^0 \rightarrow J/\psi \phi)} = (26.4 \pm 2.7 \pm 2.4)\%. \quad (2)$$

The systematic uncertainty on R has several contributions listed in Table I. The largest source of uncertainty is the f_2'

TABLE I. Systematic uncertainties on R .

| Source | Change (%) |
|--|------------|
| f_2' width | 6.3 |
| Helicity | 4.0 |
| Relative efficiency | 2.6 |
| S wave under ϕ | 2.3 |
| K^+K^- mass dependent efficiency | 2.3 |
| Background shape | 1.3 |
| \bar{B}_s^0 p_T distribution | 0.5 |
| \bar{B}_s^0 mass resolution | 0.5 |
| PID | 1.0 |
| Signal shape | 1.0 |
| $\mathcal{B}(f_2'(1525) \rightarrow K^+K^-)$ | 2.5 |
| $\mathcal{B}(\phi \rightarrow K^+K^-)$ | 1.0 |
| Total | 9.2 |

width. The error quoted reflects changing the width by 1 standard deviation from the fitted value of 90 MeV. The helicity amplitudes of the $J/\psi f_2'$ decay are unknown, unlike the $J/\psi \phi$ amplitudes which are well measured [11]. The difference between the values obtained using helicity zero and helicity one J/ψ MC samples is 4% compared to our central value. The S -wave subtraction of the events in the $J/\psi \phi$ region causes a 2.3% uncertainty. We include an uncertainty for the efficiency as a function of K^+K^- mass, as the tracking could be sensitive to the opening angle of the kaon pair. Modifying the acceptance from a flat to linear function of mass changes the yield by 2.3%. Varying the \bar{B}_s^0 p_T distribution within limits imposed by the data results in a small 0.5% change in the rate. Changing the mass resolution by its error results in a 0.5% change. A PID uncertainty of 1% is added to account for different momentum distributions of the kaons in the two final states. As a check we note that the ratio of the number of events in $J/\psi \phi$ with tight cuts to loose cuts on the kaon identification is $(61 \pm 2)\%$ and the simulation gives a consistent $(60 \pm 1)\%$. Variation of the background and signal shapes makes small differences.

In conclusion, we have made the first investigation of the $\bar{B}_s^0 \rightarrow J/\psi K^+K^-$ final state over the entire range of K^+K^- mass. There is a significant nonresonant component that extends under the ϕ region which can affect CP violation measurements [5]. We have also observed $\bar{B}_s^0 \rightarrow J/\psi f_2'(1525)$ decays. The branching fraction ratio relative to $J/\psi \phi$ is

$$\frac{\mathcal{B}(\bar{B}_s^0 \rightarrow J/\psi f_2'(1525))}{\mathcal{B}(\bar{B}_s^0 \rightarrow J/\psi \phi)} = (26.4 \pm 2.7 \pm 2.4)\%, \quad (3)$$

assuming that the background does not interfere with the signal amplitude. This decay mode can also be used to measure CP violation in the \bar{B}_s^0 system, although a different transversity analysis than in $J/\psi \phi$ would be required as the final state is a combination of a spin-1 J/ψ and a

spin-2 f_2' state. Some consideration has been given to measuring CP violation in vector-tensor decays [14].

We express our gratitude to our colleagues in the CERN accelerator departments for the excellent performance of the LHC. We thank the technical and administrative staff at CERN and at the LHCb institutes, and acknowledge support from the National Agencies: CAPES, CNPq, FAPERJ, and FINEP (Brazil); CERN; NSFC (China); CNRS/IN2P3 (France); BMBF, DFG, HGF and MPG (Germany); SFI (Ireland); INFN (Italy); FOM and NWO (the Netherlands); SCSR (Poland); ANCS (Romania); MinES of Russia and Rosatom (Russia); MICINN, XuntaGal and GENCAT (Spain); SNSF and SER (Switzerland); NAS Ukraine (Ukraine); STFC (United Kingdom); NSF (USA). We also acknowledge the support received from the ERC under FP7 and the Region Auvergne.

^aP. N. Lebedev Physical Institute, Russian Academy of Science (LPI RAS), Moscow, Russia.

^bUniversità di Bari, Bari, Italy.

^cUniversità di Bologna, Bologna, Italy.

^dUniversità di Cagliari, Cagliari, Italy.

^eUniversità di Ferrara, Ferrara, Italy.

^fUniversità di Firenze, Firenze, Italy.

^gUniversità di Urbino, Urbino, Italy.

^hUniversità di Modena e Reggio Emilia, Modena, Italy.

ⁱUniversità di Genova, Genova, Italy.

^jUniversità di Milano Bicocca, Milano, Italy.

^kUniversità di Roma Tor Vergata, Roma, Italy.

^lUniversità di Roma La Sapienza, Roma, Italy.

^mUniversità della Basilicata, Potenza, Italy.

ⁿLIFAELS, La Salle, Universitat Ramon Llull, Barcelona, Spain.

^oHanoi University of Science, Hanoi, Viet Nam.

- [1] R. Aaij *et al.* (LHCb collaboration), *Phys. Lett. B* **707**, 497 (2012).
- [2] R. Aaij *et al.* (LHCb collaboration), [arXiv:1112.3183](#).
- [3] V.M. Abazov *et al.* (D0 collaboration), [arXiv:1109.3166](#).
- [4] T. Aaltonen *et al.* (CDF collaboration), [arXiv:1112.1726](#).
- [5] S. Stone and L. Zhang, *Phys. Rev. D* **79**, 074024 (2009).
- [6] A. Alves, Jr. *et al.* (LHCb collaboration), *JINST* **3**, S08005 (2008).
- [7] R. Aaij *et al.* (LHCb collaboration), *Eur. Phys. J. C* **71**, 1645 (2011).
- [8] T. Sjöstrand, S. Mrenna, and P.Z. Skands, *J. High Energy Phys.* **05** (2006) 026.
- [9] S. Agostinelli *et al.*, *Nucl. Instrum. Methods Phys. Res., Sect. A* **506**, 250 (2003).
- [10] R. Mizuk *et al.* (Belle collaboration), *Phys. Rev. D* **80**, 031104 (2009).
- [11] K. Nakamura *et al.* (Particle Data Group), *J. Phys. G* **37**, 075021 (2010).
- [12] B. Aubert *et al.* (BABAR collaboration) *Phys. Rev. D* **79**, 112001 (2009).
- [13] R. Mizuk *et al.* (Belle collaboration) *Phys. Rev. D* **78**, 072004 (2008).
- [14] C. Sharma and R. Sinha, *Phys. Rev. D* **73**, 014016 (2006).